

ENERGY DEPOSITION AND HARD X-RAY SOURCE MOTIONS IN THE 2002 JULY 23 γ -RAY FLARE

M. D. FIVIAN, S. KRUCKER, AND R. P. LIN

Space Sciences Laboratory, University of California, Berkeley, CA 94720-7450, USA; mfivian@ssl.berkeley.edu
 Received 2008 March 28; accepted 2009 April 29; published 2009 May 20

ABSTRACT

Reconnection models of solar flares predict a systematic motion of hard X-ray (HXR) footpoints as magnetic energy is released and electrons are accelerated. While the correlation of the HXR flux with the apparent motion of the footpoints has previously been investigated, we derive and investigate for the first time the correlation between cumulative deposited energy at the footpoints and their separation. Providing excellent statistics, data from the Reuven Ramaty High Energy Solar Spectroscopic Imager of the 2002 July 23 flare are re-analyzed. The data show an excellent correlation for most of the time intervals. However, despite the good correlation, for some time ranges the derived amount of released magnetic energy is far too small to account for the energy in HXR-producing electrons.

Key words: acceleration of particles – Sun: flares – Sun: X-rays, gamma-rays

1. INTRODUCTION

Hard X-ray (HXR) bursts produced by bremsstrahlung emission of flare-accelerated electrons are the most common signatures of electron acceleration in solar flares, and provide key diagnostics for the acceleration process (e.g., Brown 1971). The intensity of the observed HXR emission indicates that a large fraction of the energy release in solar flares goes into energetic electrons with energies in the tens of keV range (e.g., Kontar et al. 2008). The magnetic energy stored in the solar corona is generally accepted to be the source of the flare energy, and magnetic reconnection processes are likely playing a key role in the energy release (e.g., Priest & Forbes 2002). The details of how so many electrons are accelerated on such short timescales are not understood.

Solar HXR bremsstrahlung from energetic electrons accelerated in the impulsive phase of a flare is observed to be primarily from the footpoints of magnetic loops (e.g., Hoyng 1981), although much fainter coronal emission is frequently present as well (e.g., review by Krucker 2008). Standard magnetic reconnection models predict increasing separation of the footpoints during the flare (e.g., Priest & Forbes 2002) as longer and larger loops are produced (see Figure 1). If the reconnection process accelerates electrons (e.g., Øieroset et al. 2002), the HXR footpoints should show this motion. The motion is only apparent; it is due to the HXR emission shifting to footpoints of neighboring newly reconnected field lines. Hence, the speed of footpoint separation together with the magnetic field strength reflects the rate of magnetic reconnection.

The inflow of magnetic energy into the reconnection region can be expressed by the inflow of Poynting flux through the area of the reconnection region by writing the energy release rate H as

$$H = 2 \frac{B_{\text{corona}}^2}{4\pi} v_{\text{in}} A_r, \quad (1)$$

where A_r is the area and v_{in} is the inflow velocity through this area (e.g., Isobe et al. 2002). Note that the factor 2 results from assuming symmetric inflow from both sides into the reconnection region.

The magnetic field in the corona, B_{corona} , and the inflow velocity, v_{in} , are very difficult to observe. More easily observable are the motion of the footpoints of the reconnected loops, v_{fp} ,

seen in HXR and the magnetic field at the photosphere B_{fp} . Using conservation of magnetic flux

$$B_{\text{corona}} v_{\text{in}} = B_{\text{fp}} v_{\text{fp}}, \quad (2)$$

the energy release rate (Equation 1) can be written as

$$H = 2 \frac{B_{\text{corona}}}{4\pi} B_{\text{fp}} v_{\text{fp}} A_r. \quad (3)$$

This energy release rate derived from the energy inflow into the reconnection region gives an upper limit for the energy deposition rate at the footpoints.

Assuming $B_{\text{corona}} \propto B_{\text{fp}}$ the product $B_{\text{fp}}^2 v_{\text{fp}}$ should therefore be roughly proportional to the energy deposition rate in the footpoints. For a constant slope of the nonthermal HXR spectrum (H becomes proportional to the HXR flux) and a constant magnetic field at the footpoints, v should be proportional to the total HXR emission from the footpoints.

Footpoint motions have been extensively studied since HXR imaging became available (e.g., Sakao et al. 1998; Qiu et al. 2002; Fletcher & Hudson 2002; Krucker et al. 2003, 2005; Asai et al. 2004; Liu et al. 2004; Grigis & Benz 2005; Temmer et al. 2007; Lee & Gary 2008; Yang et al. 2009). Systematic footpoint motions are frequently observed as expected from standard reconnection models, but often more complex behaviors are seen as well. In particular, the motion is not only seen perpendicular to the flare ribbons as predicted in a standard model with separating motion, but frequently motions along the ribbon are detected (e.g., Grigis & Benz 2005; Lee & Gary 2008). In some cases, the motion is clearly correlated with the HXR flux supporting the magnetic reconnection picture (e.g., Krucker et al. 2003), but again it is not observed for all events (e.g., Qiu et al. 2002). Asai et al. (2004) and Temmer et al. (2007) derived magnetic reconnection rates from Halpha ribbon motions and photospheric magnetic flux measurements, finding that HXR footpoints are found at a location where the derived reconnection rates are the highest. Furthermore, the variations of the reconnection rate along the Halpha ribbon are large enough to explain why significant HXR emissions are seen only from specific locations along the Halpha ribbons, but not all along the Halpha ribbon, at least for the few flares studied in detail.

In this paper we revisit the large γ -ray flare of 2002 July 23 (Figure 2) observed by the Reuven Ramaty High Energy Solar

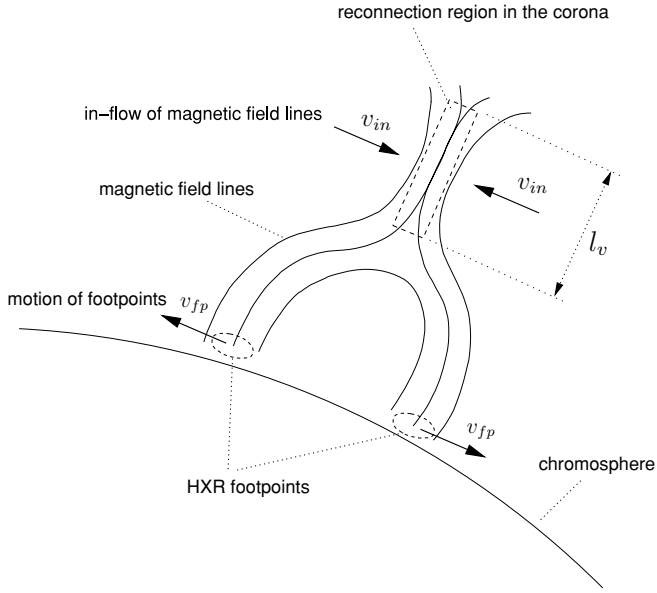


Figure 1. General scenario of magnetic reconnection in solar flares. While more and more magnetic field lines are flowing into the reconnection region magnetic energy is released. A large fraction of this energy is used to accelerate particles. These particles are traveling along the magnetic fieldlines and are producing HXR bremsstrahlung (X-rays) at the footpoints in the chromosphere.

Spectroscopic Imager (RHESSI; Lin et al. 2002) and previously studied by Krucker et al. (2003). In this event, the HXR footpoint on one of the ribbons moves systematically and the motion roughly correlates with the time variation seen in the HXR flux. This is consistent with magnetic reconnection if a higher rate of reconnection of field lines (resulting in a higher footpoint speed) produces more energetic electrons per unit time and therefore more HXR emission. The HXR emission of the second ribbon, however, shows several sources that do not seem to move systematically for more than half a minute, with different sources dominating at different times. This is inconsistent with simple reconnection models. It can be explained if the magnetic configuration is more complex and consecutively reconnected field lines have occasionally footpoints that are not located near each other but are separated by a few arcsecs resulting that the HXR emission appears to jump by the same amount.

In contrast to Krucker et al. (2003) where the HXR flux is compared with the footpoint velocity, in this work the cumulative deposited energy is correlated with the footpoint separation in order to account for spectral changes. This new approach provides two main improvements to the data analysis presented in Krucker et al. (2003): (1) using the cumulative deposited energy instead of the HXR flux takes spectral variations into account; (2) the footpoint separation does not need a differentiation as for the footpoint velocity.

2. CORRELATION

In a simple reconnection model the energy deposition rate is supposed to be proportional to the product of the magnetic field in the reconnection region, the magnetic field in the footpoints, and the velocity of the footpoint separation as described in Equation (3) in Section 1. The numerical differentiation that is needed to derive the velocity v_{fp} introduces large uncertainties, especially in the case of the measured footpoint separation, as shown in Figure 3.

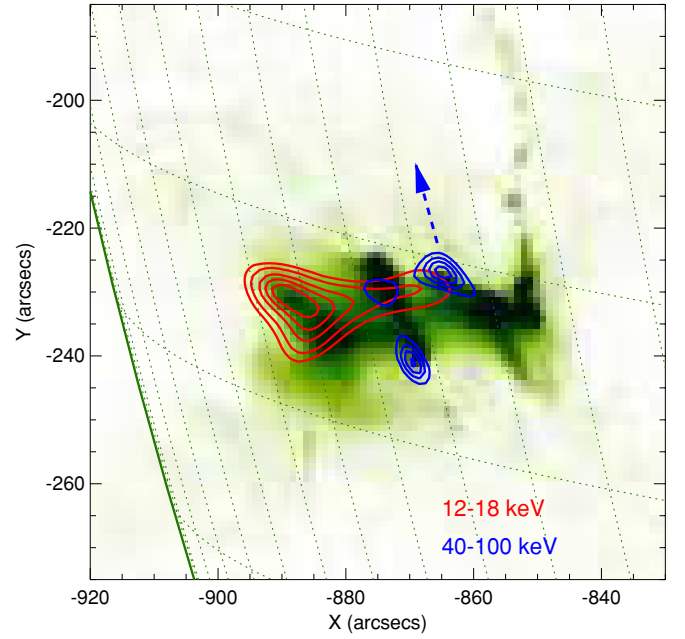


Figure 2. HXR imaging during the main peak (00:27:40-00:28:28 UT) of the impulsive phase of the 2002 July 23 flare: Contours in the thermal (12–18 keV, red) and nonthermal (40–100 keV, blue) HXR range are overlaid on a TRACE 195 Å images taken at 00:27:27UT. The arrow indicates the analyzed footprint with its approximate direction of motion. For details of source motions, see Krucker et al. (2003).

Integrating Equation (3),

$$\int_{t_1}^{t_2} H dt = \frac{1}{2\pi} \int_{t_1}^{t_2} B_{\text{corona}} B_{fp} v_{fp} A_r dt, \quad (4)$$

leads to the difference equation

$$\Delta E \equiv E(t_2) - E(t_1) = \frac{1}{4\pi} (s(t_2) - s(t_1)) \cdot B_{\text{corona}} B_{fp} A_r, \quad (5)$$

where the cumulative (or total) deposited energy $E = \int H dt$ and the footpoint separation $s = \int 2v_{fp} dt$, assuming that the magnetic field and the reconnection area are constant in time. Corresponding Equations (4) and (5) can be derived for each footpoint separately. For the here derived formalism however, we assume equivalent properties for the two footpoints.

The power-law index of the nonthermal sources is between 2.5 and 3.5 during the main HXR peaks (Holman et al. 2003). The cutoff energy is difficult to determine because of strong thermal emission and therefore, it is set to 30 keV as an upper limit. Figure 3 (panels (c) and (d)) shows the time series of the energy deposition rate with a cutoff energy set to 30 keV and its integral, i.e., the total deposited energy. It suggests a total deposited energy of $\approx 10^{31}$ erg, a typical value for an X-class flare (e.g., Holman et al. 2003; Saint-Hilaire & Benz 2005). Since the fitted cutoff energy is only an upper limit those values for the deposited energy are lower limits.

Only a certain fraction α of the energy inflow into the reconnection region is used to accelerate electrons in a downward direction and can therefore be observed in the HXR Bremsstrahlung at the footpoints. With $\Delta E_{\text{HXR}} = \alpha \cdot \Delta E$,

$$\frac{\Delta E_{\text{HXR}}}{\Delta s} = \frac{1}{4\pi} B_{\text{corona}} B_{fp} l_v l_h \alpha \quad (6)$$

according to Equation (5) with the reconnection area $A_r = l_v l_h$, where l_v characterizes the vertical (or radial) dimension of

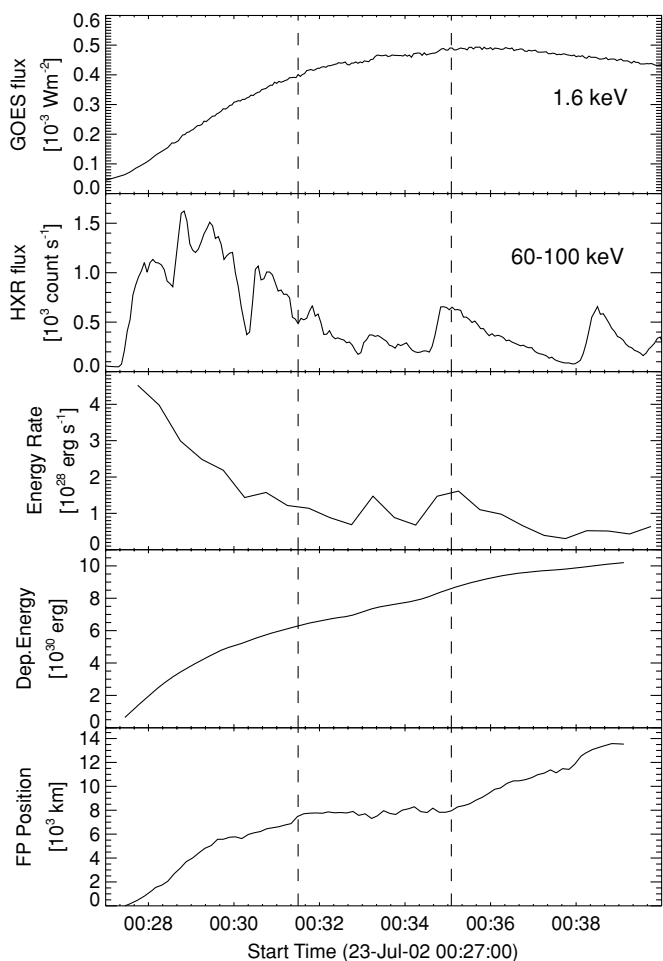


Figure 3. Time series of (a) GOES SXR flux, (b) RHESSI HXR flux, (c) energy deposition rate as derived from RHESSI spectra, (d) cumulative, total deposited energy, and (e) relative footpoint position. The vertical dashed lines indicate the time interval within which the footpoints are essentially not moving while still a lot of energy is deposited in the footprint.

the reconnection area and l_h its horizontal dimension. With ΔE_{HXR} being the measured total deposited energy and Δs being the measured separation of the footpoints, the fraction $\alpha = \alpha_{\text{accel}} \cdot \alpha_{el} \cdot \alpha_{\text{down}}$, where α_{accel} is the fraction of energy used to accelerate particles (as opposed to direct thermal heating), α_{el} is the fraction of energy used to accelerate electrons (as opposed to ions), and α_{down} the fraction of particle accelerated downward. Assuming that those three factors are in the order of one half, then α is in the order of 0.1. While α could be much smaller than that, $\alpha = 0.1$ is assumed for the analysis below. We also assume that this fraction α is constant in time and therefore has no influence on the relation between footpoint separation and observed energy deposition.

3. OBSERVATION

The intense solar flare of the GOES class X4.8 which occurred on 2002 July 23 at S13E72 has been extensively investigated (e.g., Lin et al. 2003). This two ribbon X-flare shows a HXR footprint on the western ribbon (Figure 2) that moves systematically over 15 minutes and several sources on the other ribbon that move systematically only over ≈ 30 s or less. For the northern footprint with a long duration systematic motion, Krucker et al. (2003) found a rough correlation between the HXR flux and the velocity of the motion, consistent with mag-

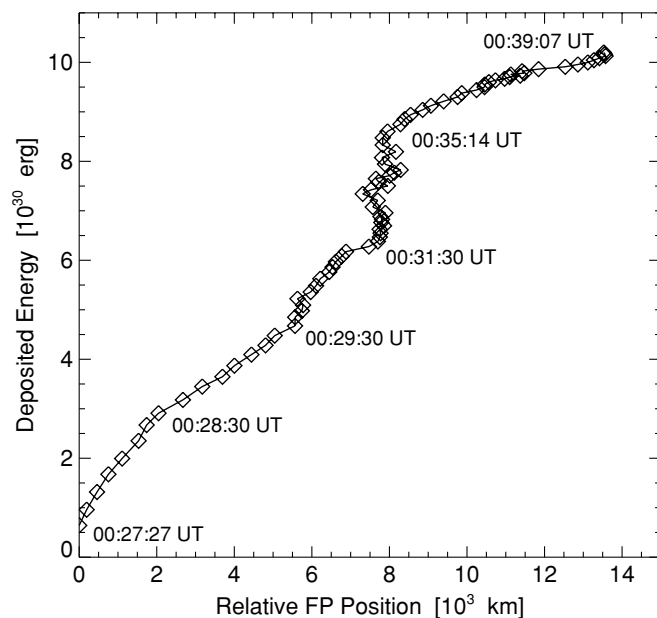


Figure 4. Correlation plot of cumulative deposited energy vs. relative footpoint position for the 2002 July 23 event shows a clear linear correlation for four time intervals. However, the observed footpoint seems essentially not moving while still a substantial amount of energy is deposited for the interval between 00:31:30 and 00:35:05 UT.

netic reconnection theory assuming a HXR spectrum constant in time (Section 1). However, the spectrum is not constant in time (Holman et al. 2003) and shows even systematic spectral differences between the two footpoints (Emslie et al. 2003). Taking the spectral variations into account, the correlation found by Krucker et al. (2003) could even improve.

In this paper we revisit the footpoint motion by testing the formalism described with Equation (6). While the systematic motion of the coronal source carries also information about the reconnection process, the motion is more complex as it is composed of emission from direct heating, nonthermal emission, and heating through chromospheric evaporation. Therefore, it cannot be directly interpreted using the above discussed formalism. For the observed motion of the coronal source, we refer to Krucker et al. (2003).

Since only one footprint shows a systematic motion, only this footprint is considered. Instead of measuring the footpoint separation, the relative position of the footprint is determined. This footprint is moving almost on a straight line in a north-northeasterly direction (see Krucker et al. 2003) and, therefore, only the motion along this line is considered. Although the individual HXR footprints show slightly different spectra, their temporal variations are closely related (Emslie et al. 2003). To simplify the data analysis, it can therefore be assumed that half of the total deposited energy derived from the spatially integrated spectrum is seen in each footprint, without introducing a time-dependent error.

Figure 4 shows the correlation plot of the cumulative deposited energy versus relative footpoint position. For the time intervals between 00:27:30 and 00:31:30 UT and between 00:35:15 and 00:39:00 UT, Figure 4 shows at least four subintervals with a clearly linear correlation between the deposited energy ΔE_{HXR} and the relative footpoint position Δs . Times with constant slope imply that the right hand side of Equation (6) is kept constant. We estimate $\Delta E_{\text{HXR}}/\Delta s \approx 8 \times 10^{21} \text{ erg cm}^{-1}$ for the earlier time interval (averaged over the three subintervals

with separate linear correlations) and $\Delta E_{\text{HXR}}/\Delta s \approx 3 \times 10^{21} \text{ erg cm}^{-1}$ for the later time interval. As many parameters in Equation (6) can vary in time, the linear correlation and the sudden slope changes are rather surprising. Whether all parameters are constant or whether they work together to keep $\Delta E_{\text{HXR}}/\Delta s$ constant is not clear.

Evaluating the right side of Equation (6), the vertical length l_v of the reconnection area can be estimated by using reasonable estimates for B_{fp} , B_{corona} and l_h . The MDI magnetogram shows a maximum of $B = 600 \text{ G}$ along the line of sight. Therefore, estimated values of $B_{\text{fp}} = 1000 \text{ G}$ and $B_{\text{corona}} = B_{\text{fp}}/5 = 200 \text{ G}$ are assumed. The horizontal dimension is assumed to be comparable to the diameter of the footpoint along the ribbon and is set to $l_h = 7 \text{ arcsec}$. These assumptions lead to an estimate of the vertical length of the reconnection area $l_v \approx 13\alpha^{-1} \text{ arcsec}$ for the earlier time interval. As described in Section 2, the factor α denotes the fraction of measured deposited energy in the footpoints with respect to the energy inflow into the reconnection area. For $\alpha = 0.1$, the vertical length of the reconnection area (see Figure 1) is estimated to be $l_v \approx 130 \text{ arcsec}$ for the earlier time interval and $l_v \approx 45 \text{ arcsec}$ for the later time interval assuming B_{fp} , B_{corona} , and l_h are the same for both intervals. Similar values of $l_v \approx 130 \text{ arcsec}$ for both intervals can be derived by assuming $B_{\text{fp}} = 400 \text{ G}$ and $B_{\text{corona}} = 80 \text{ G}$ for the second interval.

During the time interval between 00:31:30 and 00:35:00 UT however, while still a lot of energy is deposited in the footpoint, its motion seems to be essentially absent, even though a small motion perpendicular to the main direction has been observed (Krucker et al. 2003). This results in $l_v \approx 500 \text{ arcsec}$ by making the same assumption as above, but setting $\alpha = 1$ to get a lower limit for l_v . On the other hand, assuming a similar geometry as for the other time intervals, the magnetic field needed to be one order of magnitude stronger ($B_{\text{corona}} \approx 2000 \text{ G}$). Both interpretations seem to be rather unlikely.

4. CONCLUSION

The correlation shown in Figure 4 is among the best evidences that HXR source motions are correlated with the energy release in solar flares. The observed HXR footpoint motion is only partially congruent with the prediction of simple (two-dimensional) reconnection models as the correlation is only observed during some time intervals. Although these observations confirm some aspects of the simple reconnection model in a magnetic cusp, they highlight the flare energy problem. Even when using a con-

servative value of 30 keV for the cutoff energy, a large value of $\alpha = 0.1$, and a large coronal field strength ($B = 200 \text{ G}$), the needed Poynting inflow into the reconnection region is rather high and large radial sizes of the reconnection inflow region are required. Recent observations by Kontar et al. (2008) could not find evidence for a cutoff in flare photon spectra, strongly suggesting that the cutoff energies in flares are below $\approx 12 \text{ keV}$. Furthermore, the value of α is not known, and could be much lower than what is assumed here. Therefore, the deposited energies observed in the footpoints have the tendency of being rather large compared to possible values of the Poynting flux into the reconnection inflow region. Whether the assumed thick target model is overestimating the deposited energy (e.g., Kontar & Brown 2006a, 2006b; Fletcher & Hudson 2008) or some other processes besides the magnetic reconnection are feeding the energy balance is yet to be determined.

REFERENCES

- Asai, A., Yokoyama, T., Shimojo, M., Masuda, S., Kurokawa, H., & Shibata, K. 2004, *ApJ*, **611**, 557
- Brown, J. C. 1971, *Sol. Phys.*, **18**, 489
- Emslie, A. G., Kontar, E. P., Krucker, S., & Lin, R. P. 2003, *ApJ*, **595**, L107
- Fletcher, L., & Hudson, H. S. 2002, *Sol. Phys.*, **210**, 307
- Fletcher, L., & Hudson, H. S. 2008, *ApJ*, **675**, 1645
- Grigis, P. C., & Benz, A. O. 2005, *ApJ*, **625**, L143
- Holman, G. D., Sui, L., Schwartz, R. A., & Emslie, A. G. 2003, *ApJ*, **595**, L97
- Hoyng, P., et al. 1981, *ApJ*, **246**, L155
- Isobe, H., Yokoyama, T., Shimojo, M., Morimoto, T., Kozu, H., Eto, S., Narukage, N., & Shibata, K. 2002, *ApJ*, **566**, 528
- Kontar, E. P., & Brown, J. C. 2006a, *Adv. Space Res.*, **38**, 945
- Kontar, E. P., & Brown, J. C. 2006b, *ApJ*, **653**, L149
- Kontar, E. P., Dickson, E., & Kašparová, J. 2008, *Sol. Phys.*, **252**, 139
- Krucker, S., Fivian, M. D., & Lin, R. P. 2005, *Adv. Space Res.*, **35**, 1707
- Krucker, S., Hurford, G. J., & Lin, R. P. 2003, *ApJ*, **595**, L103
- Krucker, S., et al. 2008, *A&AR*, **16**, 155
- Lee, J., & Gary, D. E. 2008, *ApJ*, **685**, L87
- Lin, R. P., et al. 2002, *Sol. Phys.*, **210**, 3
- Lin, R. P., et al. 2003, *ApJ*, **595**, L69
- Liu, W., Jiang, Y. W., Liu, S., & Petrosian, V. 2004, *ApJ*, **611**, L53
- Øieroset, M., Lin, R. P., Phan, T. D., Larson, D. E., & Bale, S. D. 2002, *Phys. Rev. Lett.*, **89**, 195001
- Priest, E. R., & Forbes, T. G. 2002, *A&A Rev.*, **10**, 313
- Qiu, J., Lee, J., Gary, D. E., & Wang, H. 2002, *ApJ*, **565**, 1335
- Saint-Hilaire, P., & Benz, A. O. 2005, *A&A*, **435**, 743
- Sakao, T., Kosugi, T., & Masuda, S. 1998, in *Astrophysics and Space Science Library 229, Observational Plasma Astrophysics: Five Years of YOHKOH and Beyond*, ed. T. Watanabe, T. Kosugi, & A. C. Sterling (Boston: Kluwer), 273
- Temmer, M., Veronig, A. M., Vršnak, B., & Miklenic, C. 2007, *ApJ*, **654**, 665
- Yang, Y., Cheng, C. Z., Krucker, S., Lin, R. P., & Ip, W. H. 2009, *ApJ*, **693**, 132